A comparative analysis of an EEG model and a conductance-based neural population model

Anton V. Chizhov*, Serafim Rodrigues+ and John R. Terry†

(*) A.F.Ioffe Technical Institute, 26 Politekhnicheskaya str., 194021, St.-Petersburg, Russia

(+) School of Mathematics, Loughborough University, Leicestershire, LE11 3TU, UK

(†) Department of Engineering Mathematics, University of Bristol, BS8 1TR, UK

August 1, 2006

Abstract

We consider a firing-rate based approach to modelling EEG, justifying its use by comparison with a conductance-based refractory density population model and a set of individual neurons. It is shown that stimulation of the system by applying a step-wise current, results in a sharp peak in the population activity that can be reproduced by the EEG-model. In addition the steady-state activity may also be reproduced. Similar comparisons are obtained for stimulation via oscillatory inputs.

Keywords: neuron ensemble; population model; refractory density equation; conductance-based neuron; Fokker-Planck equation; firing-rate model; EEG

1 Introduction

The highest system level of brain activity modelling occurs at the level of EEG, corresponding to the aggregated activity of large populations of excitatory cortical neurons. Many clinical studies of humans, during cognitive tasks or in the study of neurological disorders, such as epilepsy, rely on EEG and consequently the study of models that can replicate the observed phenomena is an important step towards an understanding of the brain [1], [2], [3], [4], [5]. A mathematical analysis of these models is a promising tool for understanding the dynamics, that may then be related to those obtained from an EEG of the human brain. However, a common complaint about EEG models is that they are detached from physiology and consequently bifurcation analysis of a mean-field model does not necessarily elucidate any useful information about the functioning of the human brain. The purpose of the present work is to make the first steps towards linking mean-field approaches to modelling EEG and conductance type models based upon physiology.

To this end we wish to construct a hierarchy of models describing the dynamics of a neural ensemble.

This hierarchy should be developed from a set of equations for a conductance-based description of a single neuron and ultimately give rise to a firing-rate-based EEG model. At the intermediate level of the hierarchy a continuum population model may be considered, describing the evolution of a neural ensemble in terms of neural density in a phase space of neuron state parameters.

The equation for the neural density could be described using a Fokker-Planck-Kolmogorov approach. However, since several variables are needed to describe the state of a neuron, this approach would result in multi-dimensional equation involving partial derivatives, which would prove too difficult to solve and analyze. A numerical treatment of such an approach would provide only limited advancement of existing knowledge.

It is however possible to assume that the state variables of a neuron may be paramaterized by a single variable, resulting in a one-dimensional density equation. One such choice is based on the membrane potential [6] and is suitable for modelling a neuron assuming a monotonic profile of the membrane potential between spikes. Another technique is the so-called refractory density approach which is based upon the time elapsed since the last spike (t^*) [7]. This approach has been considered in the case of simple neuron models such as integrate-and-fire or the so-called spike-response model [8]. The advantage of this technique is that it results in a low dimensional system that is amenable to mathematical analysis.

Advancing these techniques, Chizhov and co-workers proposed an application of the refractory density approach in the case of conductance-based models [9], [10], [11]. The model considered in [9] is a reduced version of a hippocampal pyramidal cell model, considering a one-compartment neuron with voltage-dependent sodium and potassium currents (I_{DR}, I_A, I_H, I_M) [Graham (1999)] as well as with an AHP-current, I_{AHP}, which described the cumulative activity of calcium-dependent currents [12],

$$\begin{aligned}
&\tfrac{\partial \rho}{\partial t} + \tfrac{\partial \rho}{\partial t^*} = -\rho H, \\
&C\left(\tfrac{\partial U}{\partial t} + \tfrac{\partial U}{\partial t^*}\right) = -I_{DR} - I_A - I_M - I_H - I_L - I_{AHP} + I_a, \\
&\tfrac{\partial x}{\partial t} + \tfrac{\partial x}{\partial t^*} = \tfrac{x_\infty(U) - x}{\tau_x(U)}, \\
&\tfrac{\partial y}{\partial t} + \tfrac{\partial y}{\partial t^*} = \tfrac{y_\infty(U) - y}{\tau_y(U)},
\end{aligned} \tag{1}$$

where C is the membrane capacity, I_L is the leakage current, I_i are the external or synaptic currents; the approximations for the ionic currents being given by I_{DR}, I_A, I_H, I_M, I_{AHP}, with corresponding synaptic conductances g_{DR}, g_A, g_H, g_M, g_{AHP}. The functions $x_\infty(U)$, $y_\infty(U)$, $\tau_x(U)$, $\tau_y(U)$ are derived from the equations for gating variables x, y and may be found in [Graham (1999)] or [9]. This model qualitatively reproduces the activity of a neural population, i.e., an infinite number of similar adaptive neurons receiving a common input and dispersed by noise. Exempler voltage traces calculated from (1) are shown in Fig.1.

The currents I_M and I_{AHP} are particularly significant, contributing to spike frequency adaptation. We may reduce this conductance-based model to a threshold version, by omitting the fast sodium current and instead inserting an explicit threshold criterion, for the sub-threshold voltage U, which is reset at

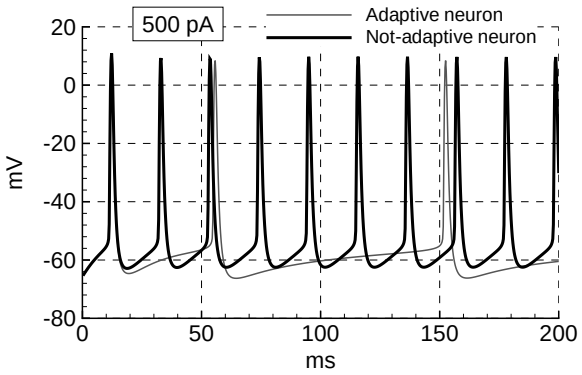

Figure 1: Voltage traces calculated by the full conductance-based model for adaptive (gray) and non-adaptive (black) neurons in the case of stimulation by step-wise current $I_a = 500$pA. The membrane area is implied to be $5.3 \cdot 10^{-4}$cm^2.

the threshold U^T, to a reset value, U^{reset}. Consideration of the sodium channel kinetics indicates that this threshold should be considered as dynamic rather than static. This may be approximated by the dependence:

$$U^T = U^T(dU/dt), \tag{2}$$

which may be calculated with the help of the full neuron model and shown in Fig.2. This reduced threshold model reproduces well both the spike timing and the voltage between spikes [5,7].

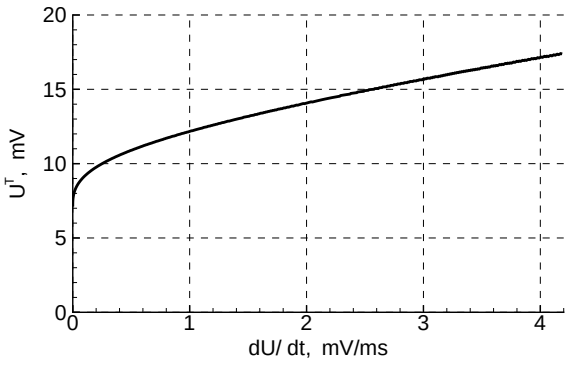

Figure 2: The threshold potential as a function of the potential slope.

The approximation for the spike-release probability density, H, is defined to be:

$$H(U(t,t^*)) = \frac{1}{\tau_m}(A(U) + B(U, dU/dt)), \tag{3}$$

where $A(U)$ is given by the curve $A = A(T)$ in Fig.3 with $T = (U^T - U)/\sqrt{2}\sigma_V$; $\tau_m = C/(g_{DR}(t,t^*) + g_A(t,t^*) + g_M(t,t^*) + g_H(t,t^*) + g_L + g_{AHP}(t,t^*))$ and

$$B(U, dU/dt) = -\sqrt{2}\ \tau_m\ \frac{dT}{dt}\ \tilde{F}(T), \qquad \tilde{F}(T) = \sqrt{\frac{2}{\pi}}\ \frac{\exp(-T^2)}{1 + \text{erf}(T)}. \tag{4}$$

This hazard function (H) defines the expected firing activity of a neuron, given the expected state of the neuron as characterized by U and dU/dt. The formula for H was derived as a result of the

sum of solutions of the Fokker-Planck equation in the two specific cases, the solution A, for the case of slow change of U, and the solution B for the case of rapidly increasing voltage. Interpreting this physiologically, the activity B arises as a result of threshold crossings by the mean membrane potential, U, whereas the activity A occurs due to threshold crossings as a result of noise-induced voltage fluctuations.

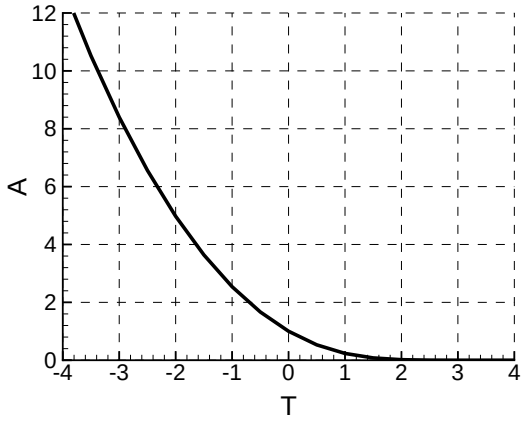

Figure 3: A component of hazard-function.

According to the single-neuron threshold model, when the potential crosses the threshold U^T, it is reset to the value $U^{\text{reset}} = -40\text{mV}$ under the assumption that this point of the repolarization phase gives $I_{Na} \approx 0$. The gating variables for the fast currents I_{DR}, I_A, I_H are also reset to fixed values, whereas the gating variables corresponding to the slow adaptation currents I_M, I_{AHP} vary dynamically and are determined by their previous state. This gives rise to boundary conditions for the potential and gating variables of the ionic currents when $t^* = 0$ of $U(t,0) = U^{reset}$, $x(t,0) = x^{reset}$, $y(t,0) = y^{reset}$, where x^{reset} and y^{reset} are

$$\text{for } I_{DR}: \quad x^{reset} = 0.262, \quad y^{reset} = 0.473; \tag{5}$$

$$\text{for } I_A: \quad x^{reset} = 0.743, \quad y^{reset} = 0.691; \tag{6}$$

$$\text{for } I_H: \quad y^{reset} = 0.002; \tag{7}$$

$$\text{for } I_M: \quad \Delta x^{reset} = 0.175 \times (1 - x(t, t^{*p})); \tag{8}$$

$$\text{for } I_{AHP}: \quad \Delta w^{reset} = 0.018 \times (1 - w(t, t^{*p})); \tag{9}$$

These values were calculated by the full model at the descending phase of a spike, when $U = U^{reset}$. For taking into account the duration of a spike the gating variables and the potential are kept constant during the time $\Delta t_{AP} = 1.5\text{ms}$. The estimation of the characteristic interspike interval, t^{*p}, is used for the adaptation currents, namely, t^{*p} is such that

$$\rho(t, t^{*p})\ H(U(t, t^{*p})) = \max_{0 < t^* < +\infty} \rho(t, t^*)\ H(U(t, t^*)).$$

The boundary condition for Eq.(1) implies that neurons return to the point $t^* = 0$ when they spike, i.e.

$$\nu(t) \equiv \rho(t,0) = \int_{+0}^{\infty} \rho H dt^*, \tag{10}$$

where $\rho(t,0)$ is the firing rate of the population. Assuming that ρ is normalized, the boundary condition (10) provides a conservation law for the number of neurons.

The firing rate calculated by the described model compares well with the activity of an infinite number of individual neurons as illustrated in Fig.4.

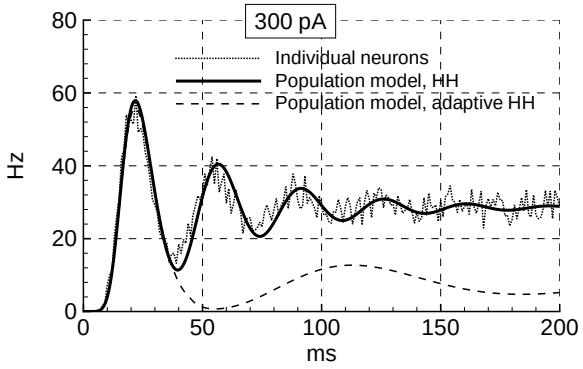

Figure 4: The transient response of the population firing rate to a rapid change in input. Beginning at $t = 0$, the excitatory input current to the uncoupled non-adapting neurons in a single population is stepped up to 300 pA. Similar simulation but taking into account the slow adaptation current I_M and both I_M and I_{AHP} is shown in dashed line. The firing rate transiently jumps up before returning to a new steady-state response. The population model firing rate (solid line) compares favourably with the averaged firing rate of individual neurons. The amplitude of noise, σ_V, is set to 2 mV.

We now proceed to consider successive reductions of the model resulting finally in a firing rate model reminiscent of the EEG-models [1], [3], [4], [5].

2 Reduction 1: Population model for LIF-neurons.

We now turn from conductance-based neurons to linear leak integrate-and-fire (LIF) neurons,

$$C\frac{dU}{dt} = -g_L(U - V_L) + I_a, \tag{11}$$
$$\text{if } \; U > U^T \; \text{ then } \; U = V^{reset},$$

with the reset fitted in order to provide reproduction of spike timing for a specific amplitude of the stimulating current (Fig.5). In this case the model provides an excellent reproduction of the spike timing for the specific amplitude of the current, however, discrepancies arise when considering different amplitudes. In addition, the model only roughly reproduces the voltage trace of a non-adaptive neuron across interspike intervals.

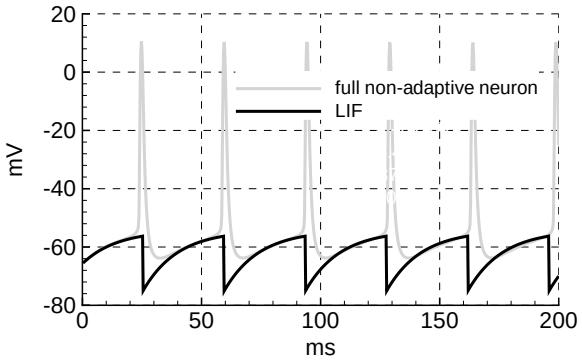

Figure 5: Voltage traces calculated by the full conductance-based model (gray) and LIF-model (black) in the case of stimulation by step-wise current $I_a = 300$ pA. The parameters of the LIF-neuron were as follows: $C = 0.37$ nF, $g_L = 25.4$ nS, $V^{reset} = -75$ mV.

The system of population model equations is now defined as follows:

$$\frac{\partial \rho}{\partial t} + \frac{\partial \rho}{\partial t^*} = -\rho H. \tag{12}$$

$$C\left(\frac{\partial U}{\partial t} + \frac{\partial U}{\partial t^*}\right) = -g_L(U - V_L) + I_a, \tag{13}$$

$$H(U(t)) = \frac{1}{\tau_m}(A(U) + B(U, dU/dt)), \tag{14}$$

$$B(U, dU/dt) = -\sqrt{2}\ \tau_m\ \frac{dT}{dt}\ \tilde{F}(T),$$

$$\tilde{F}(T) = \sqrt{\frac{2}{\pi}}\ \frac{\exp(-T^2)}{1 + \mathrm{erf}(T)},$$

$$U^T = U^T(dU/dt)$$

$A(U)$is given by the curve $A = A(T)$ in Fig.2,

$$T = (U^T - U)/\sqrt{2}\ \sigma_V, \quad \tau_m = C/g_L.$$

The **boundary conditions** are

$$\nu(t) \equiv \rho(t, 0) = \int_{+0}^{\infty} \rho H dt^*, \tag{15}$$

$$U(t, 0) = U^{reset}. \tag{16}$$

The rates calculated by the population model for the conductance-based neurons and for the LIF-neurons compare well (Fig.6) for an individual current, but differ more if the stimulating current differs from the value, at which the LIF model was fitted to the full neuron model.

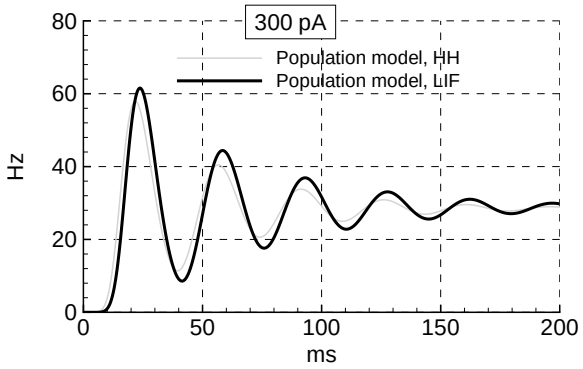

Figure 6: Population rate for the LIF-neurons (black) in the case of stimulation by step-wise current $I_a = 300$pA. To compare, the population rate calculated by the full model is shown in gray, which repeats the curve from Fig.4.

3 Reduction 2: Population model for LIF-neurons, excluding sub-threshold firing.

The terms in the approximation of the hazard-function have different physiological meanings. Recall, that the neuron voltage curve may cross the voltage threshold as a result of fluctuations due to noise, despite the mean voltage, U, being technically sub-threshold. This effect is described by the terms A in the eq.(3) or (14). The second possibility is for a genuine threshold crossing as a result of sufficient increase of the mean voltage, U. This effect was described by the term B. Typically, the term A dominates for low amplitude stimulation, whereas B dominates for strong stimulation. To demonstrate this, we consider the population firing rate omitting the term A. The result of this calculation is presented in Fig.7. Note that the model without A underestimates peaks of population rate and also it overestimates more and more the fraction of silent, sub-threshold neurons.

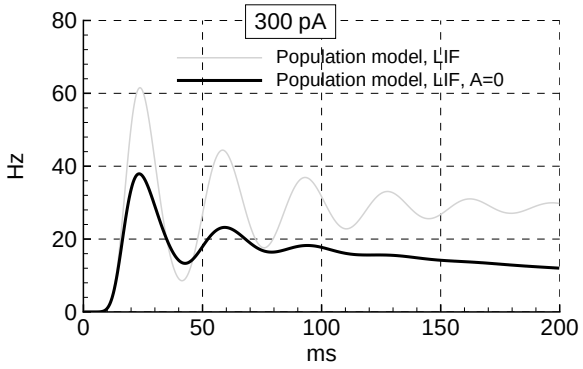

Figure 7: Population rate for the LIF-neurons without taking into account sub-threshold firing term A in the hazard-function approximation by eq.(14) (black), compared to the population rate from the model with full hazard function, shown in gray, which repeats the curve from Fig.6.

4 Reduction 3: EEG-model not distinguishing neurons by their refractory states; for LIF-neurons with fixed thresholds

Use of the partial derivative equations of the models described above is computationally expensive. Hence, to model very large scale processes, such as those recorded via EEG, we choose a very strong reduction. Specifically, we do not consider the distribution of neurons by their states between spikes. Using this assumption we now have only an ordinary differential equation for the mean potential, which describes a potential never crossing the threshold. The mean membrane potential provides the information about excitability of neurons, which is used by an analog of the hazard-function. The system of equations is defined to be

$$
\begin{aligned}
C\frac{dU}{dt} &= -g_L(U - V_L) + I_a, && (17)\\
\nu(t) &= max(A(U), B(U, dU/dt)), && (18)\\
A(U) &= \left(\tau_m\sqrt{\pi}\int\limits_{(V^{reset}-U)/\sigma_V\sqrt{2}}^{(U^T-U)/\sigma_V\sqrt{2}} e^{u^2}(1+\mathrm{erf}(u))\ du\right)^{-1}, && (19)\\
B(U, dU/dt) &= \frac{1}{\sqrt{2\pi}\sigma_V}\left[\frac{dU}{dt}\right]_+ \exp\left(-\frac{(U^T-U)^2}{2\sigma_V^2}\right), && (20)\\
\tau_m &= C/g_L, \quad U^T = const,
\end{aligned}
$$

where steady and unsteady regimes of firing are considered separately and described by the terms A and B, correspondingly. The formula for the steady-state regime was derived in [13] and can be found in [8] (see eq.(5.104)). The formula for B was derived by considering the neurons dispersed by their voltages via a Gaussian distribution about the mean, U,

$$f_G(V) = \frac{1}{\sqrt{2\pi}\sigma}\exp\frac{-(V-U)^2}{2\sigma^2}$$

Suppose that the mean voltage, $U(t)$, is monotonically increasing, then the number of neurons that have not yet fired, when compared to the total number of neurons is given by

$$\rho(t) = \int\limits_{\infty}^{U^T} g_G(V)\ dV$$

In this case the firing rate is defined to be

$$B(U(t), dU/dt) = -\frac{d\rho}{dt} = -\frac{d\rho}{dU}\frac{dU}{dt} = \frac{1}{\sqrt{2\pi}\sigma_V}\frac{dU}{dt}\exp\left(-\frac{(U^T-U)^2}{2\sigma_V^2}\right)$$

When considering only non-monotonic voltage changes in the voltage rate, dU/dt, we obtain the Eq.(20).

The comparison of this firing-rate model, which we term an *EEG-model*, with the population model is shown in Fig.8, 9A. The EEG-model gives the correct steady state (due to the term A in eq.(18)) and also reproduces the first population rate peak reasonably well for rather strong stimulation (due to the term B in eq.(18)). The subsequent peaks in the population rate are not reproducible by the EEG-model.

However, in the case of stronger noise, shown in Fig.9A, these subsequent peaks are decaying faster, thus the EEG-model being more precise in the case of a population with greater dispersion of neurons by their input currents or their intrinsic parameters. Concerning the implementation of the proposed kernel of EEG-model into a full model of interconnected populations, we note that the voltage for non-spiking neurons is known and thus synaptic currents could be introduced into the present model in a convenient way. That said, being based on a LIF-model, the EEG-model does not describe properties such as adaptation or refractoriness, as well as decreasing precision when varying stimulating current amplitudes different from the initial value at which the LIF-model was fitted to the conductance-based neuron.

In the case of oscillating input current (Fig.9B), the EEG-model is also able to reproduce at every cycle the first population spike and subsequently the average of the following population spikes.

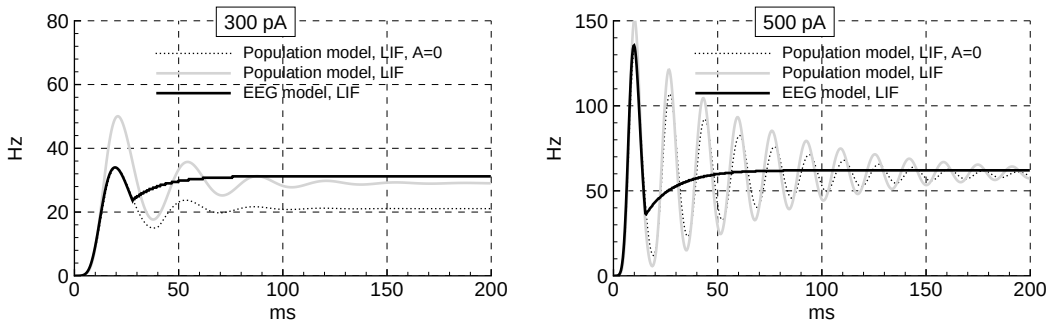

Figure 8: The EEG-model based on Eqs.17-20 is compared to the population model based on Eqs.12-16 (in grey) for two values of stimulating current amplitude. The gray curve repeats the black curve from Fig.6 and the dotted curve repeats the black curve from Fig.7.

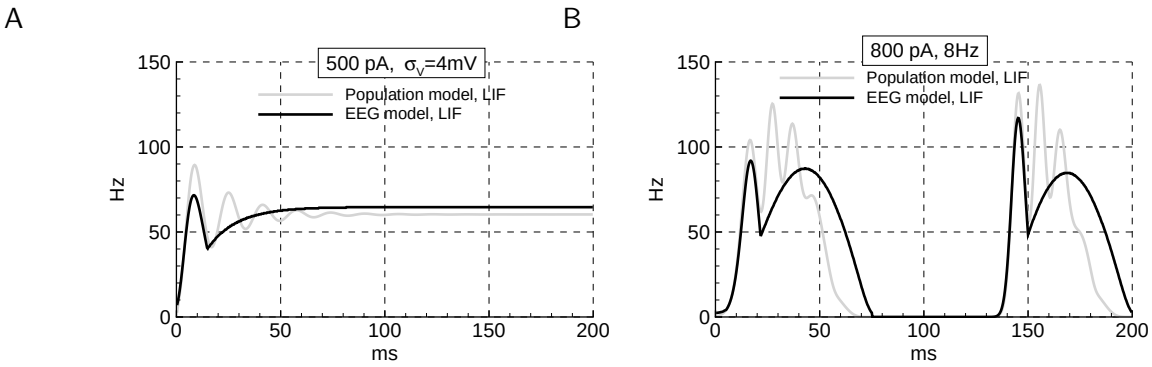

Figure 9: The EEG-model based on Eqs.17-20 is compared to the population model based on Eqs.12-16 (in grey) for larger amplitude of noise, $\sigma_V = 4$mV. *A*, step-wise input current; *B*, oscillating input current of 800pA, 8Hz.

5 Conclusion

When modelling neural activity at the level of EEG, particularly when considering epileptiform-like events, any model must be capable of reproducing at least two features. Firstly, the quasi-steady-state response

arising due to changes in incoming synaptic stimulation and secondly, the highly coherent responses observed when the stimulation rapidly excites large numbers of neurons. The proposed model is able to simulate these events, as is demonstrated by its comparison with the physiologically detailed population model, which in its turn is comparable with simulations of individual neurons. Consequently this model can be considered suitable for theoretical and clinical analysis of EEGs, as for example the study [2].

References

[1] S.Rodrigues, J.R.Terry, M.Breakspear, *On the genesis of spike-wave oscillations in a mean-field model of human thalamic and corticothalamic dynamics*, Physics Letters A **355**, 352–357 (2006).

[2] M. Breakspear, J.A.Roberts, J.R.Terry, S.Rodrigues, N.Mahant and P.A.Robinson, *A unifying explanation of primary generalized seizures through nonlinear brain modeling and bifurcation analysis*, Cereb. Cortex **10.1093**/cercor/bhj075 (2005).

[3] P.A.Robinson, C.J.Rennie, J.J.Wright, *Propagation and stability of waves of electrical activity in the cerebral cortex*, Phys. Rev. E **56**, 826–841 (1997).

[4] P.A. Robinson, C.J. Rennie, D.L.Rowe, S.C. O'Connor, *Estimation of multiscale neurophysiologic parameters by electroencephalographic means*, Human Brain Mapping **23**, 53–72 (2004).

[5] M.N.Zhadin, *Formation of rhythmic processes in the bioelectrical activity of the cerebral cortex*, Biophysics **39**, 129–147 (1994).

[6] B. Knight, *Dynamics of Encoding in a Population of Neurons*, Journal General Physiology **59** 734–766 (1972).

[7] J. Eggert, J. L. van Hemmen, *Modeling neuronal assemblies: Theory and implementation*, Neural Computation **13**, 1923–1974 (2001).

[8] W. Gerstner, W.M. Kistler, *Spiking Neuron Models Single Neurons, Populations, Plasticity*, Cambridge University Press (2002).

[9] A.V. Chizhov, L.J. Graham, *A population model of hippocampal pyramidal neurons* (submitted to Phys. Rev.E 2006).

[10] A.V. Chizhov, L.J. Graham, A.A. Turbin, *Simulation of neural population dynamics with a refractory density approach and a conductance-based threshold neuron model*, Neurocomputing (in press 2006).

[11] A.V. Chizhov A.A. Turbin, *From single-neuron models to models of neural populations*, Neuroinformatics (in Russian) **1**, 76–87 (2006).

[Graham (1999)] L. Borg-Graham, *Interpretations of data and mechanisms for hippocampal pyramidal cell models* Cereb. Cortex **13**, 19–138 (1999).

[12] N. Kopell, G.B. Ermentrout, M.A. Whittington, R.D. Traub, *Gamma rhythms and beta rhythms have different synchronization properties*, Neurobiology **97**, 1867–1872 (2000).

[13] P.I.M. Johannesma, *Diffusion models of the stochastic acticity of neurons*, In Neural Networks, 116–144, Springer (Berlin), (1968).